RECENT PROGRESS OF THE RF AND TIMING SYSTEM OF XFEL/SPRING-8*

H. Maesaka#, T. Ohshima, N. Hosoda, S. Matsubara, K. Tamasaku, T. Fukui and Y. Otake
RIKEN/SPring-8, Kouto, Sayo-cho, Sayo-gun, Hyogo, 679-5148, Japan
M. Musha, Univ. of Electro-communications, Chofugaoka, Chofu-shi, Tokyo, 182-8585, Japan

Abstract

To provide precise rf and timing signals for the XFEL facility at SPring-8, we have developed a stable optical rf and timing distribution system and a precise low-level rf control system. The phase stability of an acceleration rf field is required to be 0.1 degree (rms) of 5712 MHz, corresponding to 50 fs, and the amplitude stability is required to be 0.01% (rms). For the optical system, we use a phase-stabilized optical fiber and a water-cooled cable duct to suppress its path-length drift. In addition, the path length is monitored by an optical interferometer and regulated by a variable delay line. The phase and amplitude fluctuations of the optical system, including E/O and O/E converters were measured to be 0.71 degree (p-p[1]) and 0.86% (p-p). For the low-level rf system, we use an IQ (in-phase and quadrature) modulator to generate an acceleration rf signal and an IQ demodulator to detect the rf field. These circuits are enclosed in a water-cooled 19-inch rack to keep the temperature within ± 0.2 K. The stabilities of the rf phase and the amplitude of these instruments were measured to be 0.30 degree (p-p) and 0.56% (p-p), respectively. Although the amplitude stability is still worse than the requirement, this can be reduced by a high-power klystron that is operated at the saturation point. Consequently, the phase and amplitude stabilities are sufficient for XFEL/SPring-8.

INTRODUCTION

An x-ray free electron laser (XFEL) generates very intense and fully coherent x-rays. The brightness is 10^9-times as large as that of an existing synchrotron radiation light source. Therefore, an XFEL is one of the innovative devices for both life sciences and material sciences. In Japan, an XFEL facility is under construction at SPring-8 (XFEL/SPring-8), the construction of which is going to be completed in 2011 [1].

XFEL light is generated by a self-amplified spontaneous emission (SASE) process, as shown in Fig. 1. A high-energy electron beam is fed into an undulator beamline. The beam interacts with radiated x-rays and undulator magnetic fields, and a micro-bunch structure is formed. Since the spacing of the micro-bunch structure is the same as the x-ray wavelength, a coherent x-ray radiation is finally generated.

For the rf and timing system of an XFEL facility, the time-equivalent value of the acceleration rf phase stability must generally be less than 100 fs. Therefore, a precise low-level rf system is needed. In addition, precise synchronization over a long distance is necessary, since the facility length is at the kilometer level. For this reason, we have developed a precise rf and timing system for XFEL/SPring-8 [2].

In this paper, we describe recent progress of developing the rf and timing system of XFEL/SPring-8. After the design of the system is explained, the performance of each component is described. In particular, the stability issue is mainly discussed. The instruments introduced here can also be useful at other facilities.

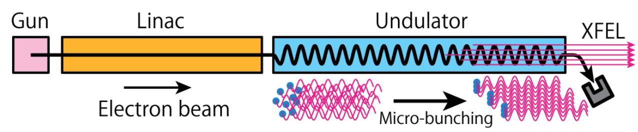

Figure 1: Schematic view of a SASE-FEL.

OVERVIEW OF XFEL/SPRING-8 AND REQUIREMENTS FOR THE RF AND TIMING SYSTEM

Figure 2 shows a schematic layout of XFEL/SPring-8. An electron beam is emitted from a CeB_6 mono-crystal thermionic electron gun and accelerated up to 8 GeV by 238 MHz, 476 MHz, 1428 MHz (L-band), 2856 MHz (S-band) and 5712 MHz (C-band) accelerating structures. The accelerating rf power is provided from a high-power klystron, which is driven by the rf and timing system. The beam is then injected into in-vacuum undulators and a XFEL light is generated.

To stimulate the SASE process, the electron beam must have a sufficiently high peak current. The required peak current of XFEL/SPring-8 is 3 kA [2]. However, the current of the gun is only 1 A. Therefore, we compress the temporal bunch length from 1 ns to 30 fs (FWHM) in order to increase the peak current. Bunch compression is done by velocity bunching in the low-energy region ($\beta<1$) and by three magnetic chicanes at the high-energy region ($\beta\sim1$). In each process, an accelerating rf field gives an energy chirp to the electron bunch, so that the energy of head electrons becomes smaller than that of tail electrons. In the velocity-bunching case, tail electrons approach head electrons. Along the magnetic chicane, higher-energy tail electrons travel shorter paths than lower-energy head electrons. Thus, the bunch length is shortened.

To achieve a stable bunch compression ratio, we need a precise rf and timing system. Since the strength of the energy chirp is very sensitive to the bunch compression,

*Work supported by Japan Science and Technology Agency (JST) and Ministry of Education, Culture, Sports, Science and Technology of Japan (MEXT).
#maesaka@spring8.or.jp
[1]peak-to-peak

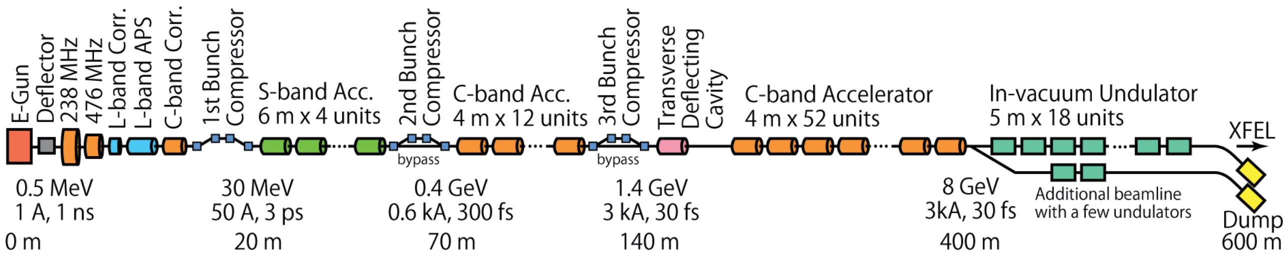

Figure 2: Schematic layout of XFEL/SPring-8.

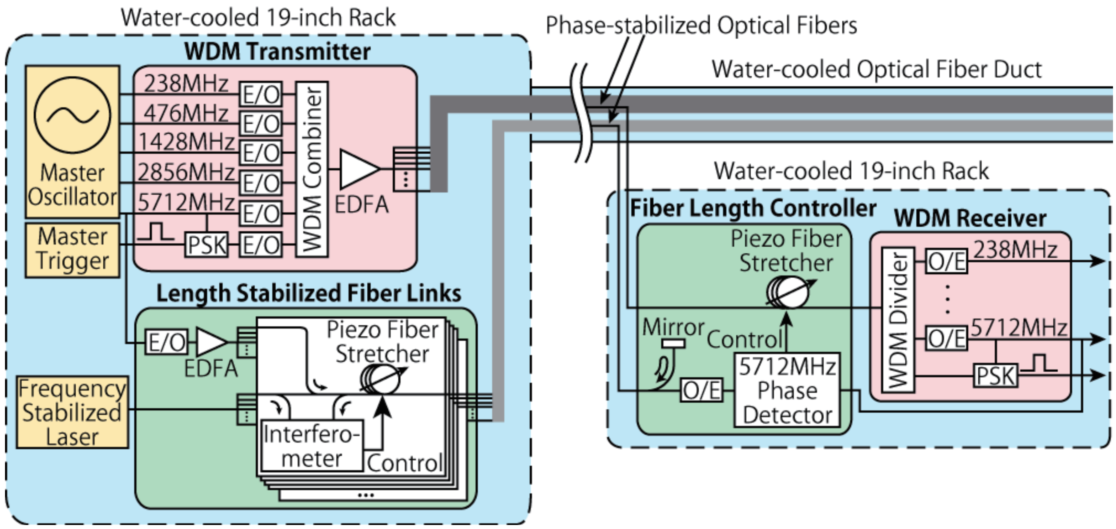

Figure 3: Block diagram of the optical rf and timing distribution system.

the phase and amplitude of the acceleration rf field must be precisely controlled. For the most severe part, the phase and amplitude fluctuations must be less than 0.1 degree (rms) of 5712 MHz, corresponding to 50 fs, and 0.01% (rms), respectively [2]. Furthermore, some experiments, such as pump-probe experiments, demand the same value for the time reference of the equipment.

In addition to the stability issue, rf and timing signals are necessary to be distributed to many accelerator units and experimental apparatus through long transmission lines. The length of the accelerator is 400 m and the distance between the gun and the experimental hall is 700 m. We use optical fibers to distribute the signal, because they have much less attenuation than metal cables. To achieve femtosecond stability, the path-length fluctuation due to temperature drift must be reduced.

DESIGN OF THE RF AND TIMING SYSTEM

Considering the accelerator configuration of XFEL/SPring-8, we designed an rf and timing system consisting of two parts. One is an optical rf and timing distribution system to provide a stable time reference rf and a trigger signal for each component; the other is a precise low-level rf control system to manipulate the phase and amplitude of the rf field for each accelerator unit. We describe the hardware design for each part.

Optical RF and Timing Distribution System

The requirements for the optical rf and timing distribution system are summarized below: (1) In total, six signals are needed: 238 MHz, 476 MHz, 1428 MHz, 2856 MHz and 5712 MHz rf signals and a trigger signal. (2) The signal must be transmitted over a long distance of up to 1 km. (3) The timing stability should be at the 50 fs (rms) level.

To fulfill these demands, we designed an optical rf and timing distribution system, as shown in Fig. 3. Rf and trigger signals are generated by a low-noise master oscillator and a master trigger generator [2,3]. Each signal is converted to a sinusoidally-modulated optical signal by an electrical-to-optical (E/O) converter consisting of a distributed feedback (DFB) laser diode and a $LiNbO_3$ modulator. The wavelength of the carrier light is approximately 1550 nm. For the trigger pulse, the signal is converted to a 5712 MHz phase shift keying (PSK) signal and then converted to an optical signal, because a low-duty cycle pulse signal is hardly to be transmitted by an optical signal. All optical signals are combined to one optical fiber by a wavelength-division multiplexing (WDM) technique. The combined signal is amplified by an erbium-doped fiber amplifier (EDFA) and distributed to each component through phase-stabilized optical fibers (PSOF). The temperature coefficient of the PSOF is 1 ps/km/K, which is much less than that of conventional optical fibers. At the receiver, the optical signal is divided according to the wavelengths; the electric rf and timing signals are obtained from a fast photo-diode in the optical-to-electrical (O/E) converter.

Length-stabilized fiber links are additionally prepared in order to compensate for the path-length fluctuation of the WDM fibers. This link transfers a frequency-stabilized laser as a length standard and a 5712 MHz rf signal as a time reference. A part of the length standard light is reflected at the receiver, and the fiber length is measured with a Michelson interferometer in the transmitter with sub-micron resolution [2,4]. The length data is fed back to a variable delay line, such as a piezo-electric fiber stretcher. The time drift of the WDM line, including all instrument drifts is monitored at the receiver side by using the rf phase detector of the 5712 MHz signal, and the fiber length is controlled with a fiber stretcher. We are also considering a possibility to use a higher rf frequency to measure the time drift more precisely.

To keep the temperatures of all the electric circuits and optical fibers, we also developed a water-cooled 19-inch rack and a water-cooled fiber duct. Details of these enclosures are described in the next section.

Precise Low-level RF Control System

To adjust the phase and amplitude of the rf field for each accelerating unit, we designed a precise low-level rf control system consisting of IQ modulators and demodulators. The output of the IQ modulator, $V(t)$, is

$$V(t) = I(t)\cos(\omega t) + Q(t)\sin(\omega t), \quad (1)$$

where ω is the angular frequency of a carrier wave and $I(t)$ and $Q(t)$ are input baseband signals of in-phase and quadrature-phase, respectively. The IQ modulator can generate any rf signals with arbitrary phase and amplitude waveforms. Conversely, the IQ demodulator receives an rf signal, and reproduces baseband IQ waveforms. This function is realized by two rf mixer ICs and a quadrature-phase power splitter.

A block diagram of the low-level rf control system is illustrated in Fig. 4. A reference rf signal from the WDM receiver is provided to the IQ modulator and a pulsed rf signal with appropriate phase and amplitude is created. IQ baseband waveforms are generated by a VME 238MHz 14-bit D/A converter board [5]. The pulse rf signal is amplified by a solid-state amplifier and a klystron, and fed into accelerating cavities. A tiny part (10^{-4}–10^{-6}) of the rf power around the accelerator cavity is picked up and detected by an IQ demodulator. The detected IQ baseband waveforms are recorded by a VME 238MHz 12-bit A/D converter board [5]. Trigger signals for the D/A and A/D converters and other devices are provided by a VME trigger delay unit (TDU). The TDU generates trigger pulses at configured timing with a small jitter of less than 1 ps [3]. To reduce slow drifts of the acceleration rf phase and amplitude, the detected signal is fed back to the D/A converter with a PID (Proportional-Integral-Derivative) feedback control algorithm.

The temperature of each module is regulated by a water-cooled 19-inch rack in the same way as the optical system. In addition, the DC power of every module is distributed from a water-cooled low-noise power supply. The purposes of this configuration are to reduce the heat load of the water-cooled 19-inch rack and to drive each circuit with a stable power source.

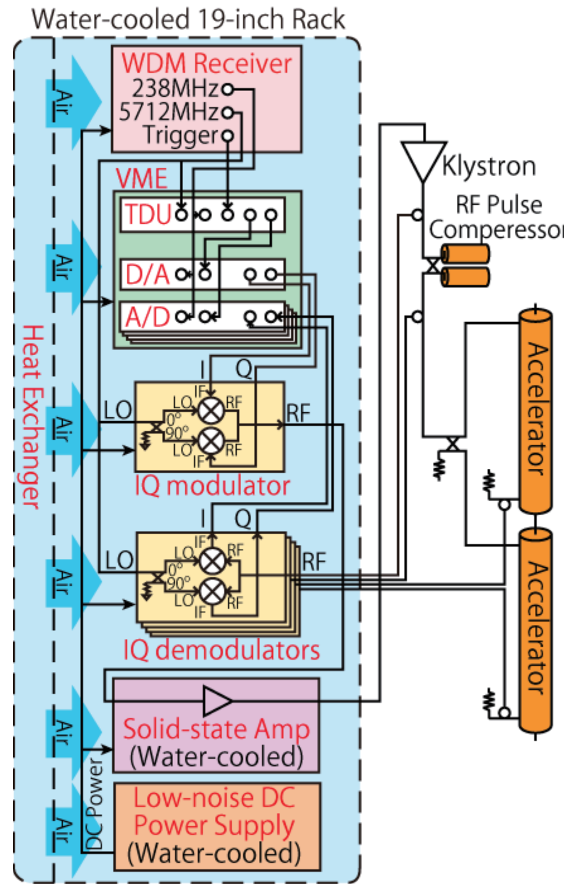

Figure 4: Block diagram of the low-level rf control system.

RECENT PROGRESS OF EACH COMPONENT

The designed system is now under mass-production. Some of the products are installed in the XFEL/SPring-8 building, as shown in Fig. 5. In this section, we firstly introduce temperature-regulated enclosures, and then describe the performance of the first product of each component.

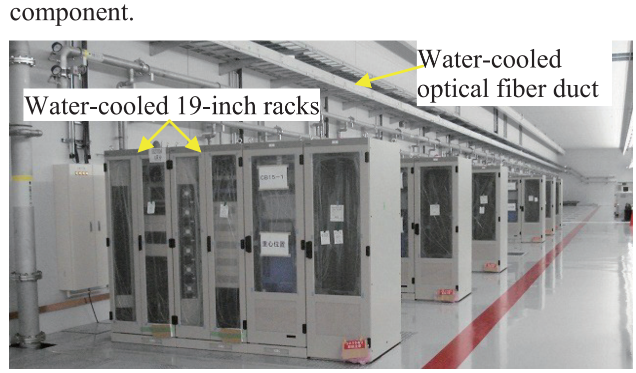

Figure 5: Photograph of the installed optical fiber duct and water-cooled 19-inch racks.

Water-cooled 19-inch Racks

To stabilize the temperature of the electrical and optical components, we developed two types of water-cooled 19-inch racks, as shown in Fig. 6. Both types are equipped with heat exchangers, which provide water-cooled air for enclosed components. The temperature stability of the cooling water from the facility is 0.4 K (p-p). The difference between the two types is the place of the air outlet. One is the side of the component and the other is the front. We use a side-blowing type for the rf and timing system to prevent the vibration of cables around the front panel. The air flow inside the enclosed rf module is carefully designed to reduce any vibration of rf cables. In addition, VME boards are horizontally mounted in order to realize smooth air flow. The front-blowing type is used for magnet power supplies and other analog circuits.

We measured the temperature stability of the water-cooled rack. In this measurement, an approximately 1 kW head load was exposed in the rack. Temperature trend graphs are plotted in Fig. 7. At the middle of the measurement, the water temperature and the outside temperature were decreased by 0.4 K and 4 K, respectively. The temperature drift of the inside was 0.42 K. Thus, the inside temperature appropriately followed the water temperature variation and was almost insensitive to the outside temperature.

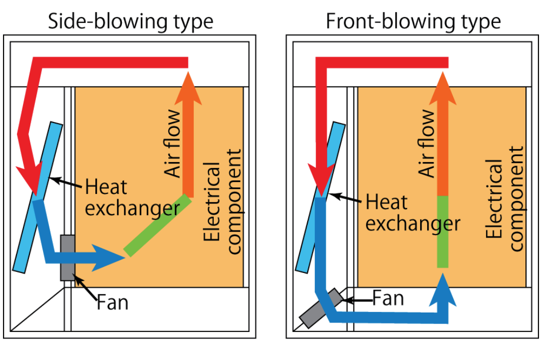

Figure 6: Schematic drawings of water-cooled 19-inch racks (top view). The left figure shows the side-blowing type and the right shows the front-blowing type.

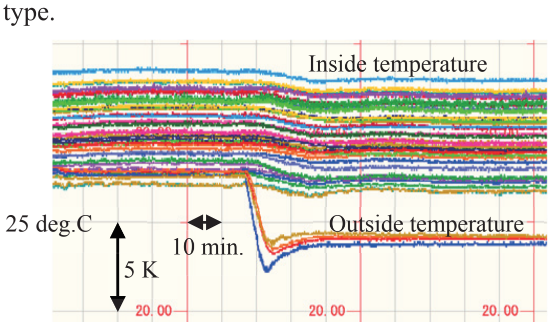

Figure 7: Trend graphs of the temperatures of inside and outside of the water-cooled 19-inch rack.

Water-cooled Optical Fiber Duct

We developed a water-cooled optical fiber duct to stabilize the fiber temperature, as shown in Fig. 8. PSOFs are inserted into a steel duct together with water pipes in which temperature-regulated water within 0.4 K (p-p) is circulated.

A prototype module of the duct was manufactured and the temperature stability was measured. Figure 9 shows the results from a measurement. Although the temperature fluctuation of the outside air was 3.4 K (p-p), the inside temperature was stabilized within 0.12 K (p-p). The stability of the cooling water temperature was 0.24 K (p-p). Consequently, the length drift of a 1km-long PSOF can be reduced to 100 fs (p-p) level.

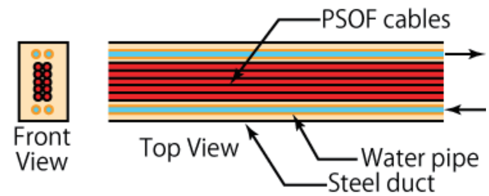

Figure 8: Schematic drawing of the water-cooled optical fiber duct.

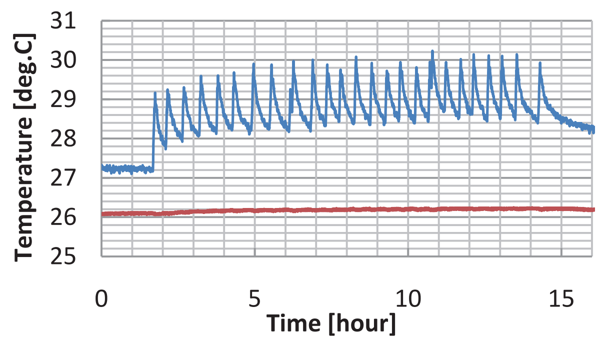

Figure 9: Trend graphs of the temperatures of inside (red) and outside air (blue).

Optical Transmitter and Receiver

The first product of a WDM optical transmission system including a transmitter and a receiver was assembled. We measured the single-sideband (SSB) phase noise of the rf signal transmitted by this system with the Agilent E5500 signal source analyzer. The transmitter and the receiver were connected with a 500m-long PSOF. The results of the measurements are shown in Fig. 10. The phase noise after signal transmission through the optical system is almost identical to that of the signal source. No noise growth can be seen below 1 MHz. Although a small deterioration is found above 1 MHz, this effect is equivalent to a timing jitter of 7 fs, which is sufficiently small. The evaluated rms time jitter according to Ref. [2] is approximately 30 fs.

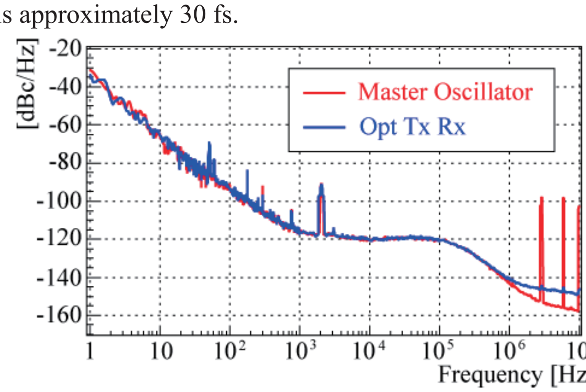

Figure 10: SSB phase noise before and after the WDM optical distributer. The blue line shows the phase noise of the 5712 MHz signal after transmission. The red line shows the phase noise of the master oscillator.

The stabilities of the phase and amplitude were also measured. In this measurement, the transmitter and the receiver were placed in a thermostatic chamber, and were connected with a short PSOF. The phase and amplitude were monitored with a network analyzer for 24 hours. The temperature variation during the measurement was 0.7 K (p-p). The trend graphs of the measurement are plotted in Fig. 11. The fluctuations of the phase and amplitude of the 5712 MHz signal were 0.71 degree (p-p) and 0.86% (p-p), respectively.

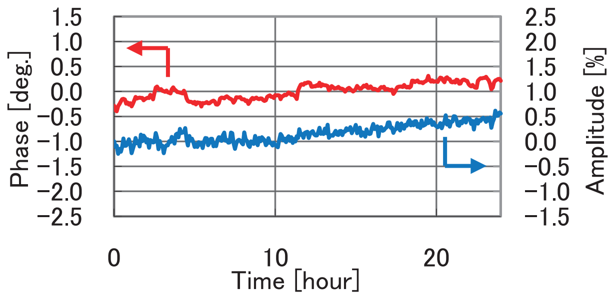

Figure 11: Trend graphs of the phase (red) and amplitude (blue) of the 5712 MHz signal after the optical rf and timing transmission system.

Precise Low-level RF Control System

The first product of the precise low-level rf control system was manufactured and the basic performance was measured. The measurement setup was almost the same as Fig. 4. Only one difference was that the output of the solid-state amplifier was directly connected to an IQ demodulator together with an attenuator. A rectangular waveform was generated by the D/A board and the phase and amplitude of the rf signal from the solid-state amplifier were recorded by the A/D board. Trend graphs of 2-hour stability data are shown in Fig. 12. The phase and amplitude fluctuations were 0.30 degree (p-p) and 0.56% (p-p), respectively. Both values are almost the measurement limit of this system.

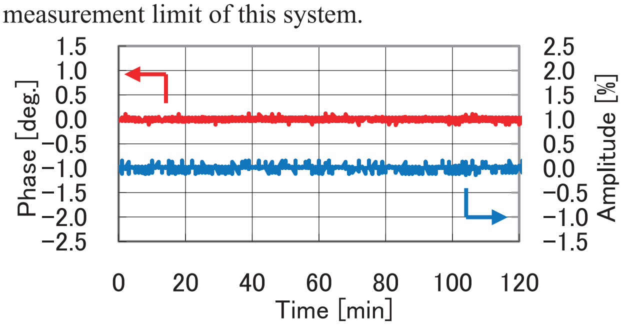

Figure 12: Trend graphs of the phase (red) and amplitude (blue) of the stability test of the 5712 MHz low-level rf control system.

In addition to the stability test, the phase and amplitude errors of the IQ modulator and demodulator were measured and corrected. Suppose that an IQ modulator has an amplitude error of 1%, for example, the output rf amplitude can change by 1%, even if only the phase is varied. This error affects the fine tuning of the accelerator, and also disturbs the feedback control of the low-level rf system because the phase feedback loop interferes with the amplitude loop and vice versa. Fortunately, this error is the characteristic of each circuit, and does not drift. Therefore, we can correct the error by software. The details of the correction method are described in Ref. [6]. The phase and amplitude errors were reduced from 6 degrees (p-p) to 0.3 degree (p-p) and from 12% (p-p) to 1% (p-p), respectively.

SUMMARY AND DISCUSSION

Since XFEL/SPring-8 demands precise rf and timing signals, we developed an optical rf and timing distribution system and a precise low-level rf control system. The required phase and amplitude stabilities are 0.1 degree (rms) of 5712 MHz and 0.01% (rms), respectively. For the optical system, low-noise rf signals generated by a master oscillator are transmitted in one optical fiber by using the WDM technique. A water-cooled optical fiber duct and a fiber length stabilization system were developed in order to reduce the fiber length drift. A water-cooled 19-inch rack was also developed to regulate the temperature of the electrical component. For low-level rf control, we developed a stable IQ modulator and demodulator system enclosed in a water-cooled rack.

We measured the stability performance of the first products. The phase fluctuations of the optical system and the low-level rf system were 0.7 degree (p-p) and 0.3 degree (p-p) of 5712 MHz, which were comparable to the demanded value. On the other hand, the amplitude fluctuation was more than 0.5% (p-p), which is larger than the requirement. However, the amplitude fluctuation could be suppressed by a klystron, which is operated at the saturation point where the output power is insensitive to the input power. Thus, we can conclude that the performance of the rf and timing system is sufficient for XFEL/SPring-8.

ACKNOWLEDGEMENTS

We thank Mitsubishi Electric Tokki System Inc. and Kinden Inc. for their great efforts to accomplish the stable rf and timing system.

REFERENCES

[1] T. Shintake, "Current Status of X-ray FEL Project at SPring-8", proceedings of FEL09 (2009).
[2] Y. Otake *et al.*, "Timing and LLRF System of Japanese XFEL to Realize Femtosecond Stability", proceedings of ICALEPCS'07 (2007).
[3] N. Hosoda *et al.*, "SCSS Prototype Accelerator Timing System", proceedings of APAC'07 (2007).
[4] M. Musha *et al.*, Appl. Phys. **B** 82, 555–559 (2006).
[5] T. Fukui *et al.*, "A Development of High-Speed A/D and D/A VME Boards for a Low Level RF System of SCSS", proceedings of ICALEPCS'05 (2005).
[6] T. Ohshima *et al.*, "Correction of Phase and Amplitude Error of RF modulator and demodulator", in these proceedings.